Published in final edited form as:
FEBS Lett. 2012 February 17; 586(4): 330–336. doi:10.1016/j.febslet.2012.01.019.

Cataract-Linked γD-Crystallin Mutants Have Weak Affinity to Lens Chaperones α-Crystallins

Sanjay Mishra, **Richard A. Stein**, and **Hassane S. Mchaourab***
Department of Molecular Physiology and Biophysics, Vanderbilt University, Nashville, TN 37232, USA

Abstract

To test the hypothesis that α-crystallin chaperone activity plays a central role in maintenance of lens transparency, we investigated its interactions with γ-crystallin mutants that cause congenital cataract in mouse models. Although the two substitutions, I4F and V76D, stabilize a partially unfolded γD-crystallin intermediate, their affinities to α-crystallin are marginal even at relatively high concentrations. Detectable binding required further reduction of γD-crystallin stability which was achieved by combining the two mutations. Our results demonstrate that mutants and possibly age-damaged γ-crystallin can escape quality control by lens chaperones rationalizing the observation that they nucleate protein aggregation and lead to cataract.

Keywords

γD-crystallin; denaturant unfolding; bimane fluorescence; αB-crystallin phosphorylation; α-crystallin; β-crystallin; chaperone; small heat-shock protein; cataract

1. Introduction

A unique cellular and molecular architecture enables the ocular lens to transmit and focus light on the retina. The lens consists of layered terminally differentiated cells, the fiber cells, which lose their organelles early in development and are unable to synthesize or turn over proteins [1]. Transparency and refractivity entail short-range order packing of highly water soluble proteins, α-, β- and γ-crystallins, which account for more than 90% of the lens protein weight [2]. A highly tuned balance of forces prevents long range order or crystallization at the high crystallin concentrations found in fiber cells [3,4].

Under assault by environmental factors, the optimized protein packing is eventually perturbed leading to protein aggregation and light scattering. The “wear and tear” of lens aging is recorded at the molecular level through accumulated modifications of the crystallins [5,6] such as truncations [7,8], glycation [9,10], oxidations [11] and deamidations [12]. In the absence of protein turn-over, loss of crystallins stability and/or solubility alters the balance of forces between proteins thereby compromising lens transparency and refractivity. Age-related cataract is an opacification of the lens which can result from protein unfolding and subsequent aggregation [1] and/or changes in the surface properties of molecules

*Corresponding Author. hassane.mchaourab@vanderbilt.edu.

leading to loss of solubility [13–15]. One of the mechanisms hypothesized to delay aggregation in the lens is the activity of resident small heat-shock proteins (sHSP) [16] αA- and αB-crystallin. In his seminal work, Horwitz proposed [17,18] that by inhibiting lens proteins aggregation, α-crystallins delay the onset of cataract. The protein unfolding hypothesis for age-related cataract posits that progressive modifications of β- and γ-crystallins reduce their free energies of unfolding and promote their binding to α-crystallin. The disappearance of soluble α-crystallin from the center of normal human lenses by age 40 [19] is hypothesized to set the stage for aggregation of destabilized proteins. Aging is characterized by a progressive shift in the molecular weight distributions of fiber cells proteins [20]. Similar to late-onset aggregation diseases, the gradual accumulation of modified proteins in the lens overwhelms the chaperone machinery.

Despite their abundance, β- and γ-crystallins do not have a defined role in lens development. They are considered structural proteins whose packing and interactions are optimized for transparency and refractivity [1]. Both β- and γ-crystallins are members of the same protein superfamily [21]. The folds of the dimeric β- and monomeric γ-crystallins consist of four greek key motifs organized in two domains [22,23]. The main sequence difference between the two families is N-terminal extensions in the β-crystallins, with the basic isoforms having additional C-terminal extensions. Seven γ-crystallins are expressed in the human lens; the most abundant, γD-crystallin, accounts for 11% of the total protein content in the fiber cells.

A number of mutations in γ-crystallins have been associated with congenital cataracts in humans and mouse models. These include “solubility mutants” where residue substitutions change the surface property of the molecule [24,25]. Another class of mutants is associated with changes in stability, i.e. shifts in the unfolding equilibrium [26,27]. Studies of two such mutants in mouse models suggest multiple mechanistic origins of cataract [26,27]. The substitution of I4F in γB-crystallin results in large inter-fiber spaces and large aggregates in the inner fiber cells [26]. Although the mutant appears to associate with α-crystallin in mouse lens extract, temperatures higher than 37 °C were required to form the complex *in vitro*. γD-crystallin mutant V76D forms intranuclear aggregates that disrupt denucleation of fiber cells [27].

The existence of cataract-causing, destabilized mutants of lens proteins poses a conundrum for the chaperone hypothesis of α-crystallin function. αA-crystallin constitutes 30% of total lens proteins and its binding capacity could reach one substrate per subunit of equivalent molecular mass [16]. Thus, either the γ-crystallin mutants are not efficiently bound by α-crystallins or γ-crystallin may have a yet undefined cellular role in lens development that is inhibited by its destabilization and subsequent interaction with α-crystallin. To distinguish between these possibilities, we investigated the interaction between both α-crystallin subunits and destabilized mutants of γD-crystallin. The experimental design follows our established approach that emphasizes a direct quantitation of binding in the absence of aggregation [28]. For this purpose, γD-crystallin mutants associated with congenital cataract in mice were constructed and their unfolding equilibrium characterized. Binding to α-crystallins was detected by changes in the fluorescence intensity and anisotropy of a bimane probe site-specifically attached to γD-crystallin. We find remarkably low affinities *in vitro* suggesting that these mutants may escape quality control by α-crystallin chaperone. These findings are interpreted in the context of the folding equilibrium of γ-crystallin and built-in repulsive interactions between crystallins critical for lens refractivity and transparency.

2. Material and methods

2.1 Expression and purification of crystallins

Human γD-crystallin was a generous gift from Dr. C. Slingsby, Birbeck College. The I4F, V76D, and I4F/V76D mutants were generated by QuikChange procedure (Stratagene). Mutagenesis was confirmed by DNA sequencing.

The proteins were expressed and purified as described by Jung et al. [29] except that γD-crystallin expression was at 25 °C for 10 h and the final gel filtration purification was carried out in Buffer A (9 mM MOPS, 6 mM Tris, 50 mM sodium chloride, 0.1 mM EDTA, 0.02% (w/v) sodium azide; pH 7.2) supplemented with 20% glycerol (v/v). Bimane was added after the second cation exchange column concurrently with pH adjustment to 7. The reactions were incubated for 2 hours at room temperature with 10× monobromobimane. The excess label was then removed by the gel filtration step. Stoichiometric labeling at cysteine, C111, was confirmed by MS/MS of intact protein as well as by MS/MS of tryptic protein fragments (data not shown). Predicted molar extinction coefficient of 43,235 $M^{-1}cm^{-1}$ was used to determine γD concentrations. αA-, αB- and the triply phosphorylated analog (S19D/S45D/S59D) of αB-crystallin, referred to as αB-D3, were purified as previously described [30–32]. Protein concentrations for αA- and αB-D3 were determined from extinction coefficients [33]: 16,507 and 19,005 $M^{-1}cm^{-1}$, respectively.

2.2 Circular Dichroism (CD) spectroscopy

Spectra were collected on a Jasco J-810 Spectropolarimeter in 20 mM phosphate buffer, pH 7.1. Near-UV spectra (330–250 nm) were obtained using a 0.5 mg/ml protein solution at room temperature. Far-UV spectra (260–185 nm) were collected at room temperature using a 0.1 mg/ml protein solution.

2.3 Binding of γD-crystallin to α-crystallin

25 μM γD-crystallin was mixed with α-crystallins at the appropriate molar ratio then incubated at 37 °C for 2 h. Bimane emission spectra were collected from 420 to 500 nm following excitation at 380 nm (Photon Technology International (PTI) L-format spectrophotometer). The fluorescence anisotropy of γD-crystallin was measured on a T-format spectrophotometer (PTI). The fluorescence intensities parallel and perpendicular to the direction of polarized light were analyzed to determine steady state anisotropy values. The samples were excited at 380 nm, and the fluorescence signal was monitored at 465 nm. Binding isotherms were generated by plotting bimane emission or anisotropy at 465 nm as a function of the [α-crystallin/γD-crystallin] ratio.

2.4 Analytical size exclusion chromatography (SEC)

Binding between bimane-labeled γD-crystallins and α-crystallins was analyzed by gel filtration on a Superose 6 10/300 GL Column (GE Healthcare Life Sciences) equilibrated in Buffer A. Samples were incubated at 37 °C for two hours prior to injection. Protein elution was monitored by tandem absorbance (280nm) and fluorescence (excitation 380nm; emission 475nm).

2.5 Thermodynamic analysis of γD-crystallin mutants

Denaturant-unfolding curves were constructed by monitoring tryptophan fluorescence of γD as a function of guanidine hydrochloride concentration. Bimane-labeled γD-crystallin constructs (5μM final concentration) were mixed with 1–5 M guanidine hydrochloride (8M stock solution in Buffer A supplemented with 1mM DTT, pH 7.2) and were incubated at 25 °C or at 37 °C for 10 h. The denaturation curves did not change upon further incubation for

up to 24 hours. The curves were fit to a three-state unfolding model [34] by nonlinear least-squares methods using the software Origin (Origin Lab).

3. Results

3.1 Methodology

The topological location of the γD-crystallin mutants, which cause congenital cataract in mice, is shown in Figure 1. I4 and V76 are located in the N-terminal domain of the molecule in a buried environment. I4F substitutes a conserved isoleucine in the first β-strand of the greek key motif by a phenylalanine. Because the mutation preserves the hydrophobic nature of the side chain, its effects on stability must be mediated by steric repacking. In contrast, the substitution of valine 76, which is located in a loop between β-strands 5 and 6, by an aspartate introduces a charged residue in the packed protein interior. Although Wang et al. [27] noted that the aspartate's carboxylate group could hydrogen bond to nearby arginine residues, this does not appear sufficient to neutralize its destabilizing effect. Finally, we have combined both mutations with the goal of further destabilizing the protein. Our model of α-crystallin chaperone activity (Scheme 1) [16] links its apparent affinity to the fractions of: 1) activated α-crystallin, $(sHSP)_a$ and [35,36] 2) partially or globally unfolded substrate (I and U in Equation 1). Thus, in comparing multiple mutants with different free energies of unfolding, their relative affinities to α-crystallin are expected to parallel reduction in the stability of the native state N.

To investigate γD-crystallin binding to α-crystallin, we selectively attached a bimane label at cysteine 111 (Figure 1). Bimane labeling marginally reduces the stability of the WT without significant changes in the shape and apparent cooperativity of the unfolding curve (Supplementary Figure 1).

3.2 Structure and unfolding equilibrium of γD-crystallin mutants

Figure 2A shows that, at room temperature, I4F and V76D substitutions do not change the overall secondary structure of γD-crystallin. The minimum at 218 nm suggests that γD-crystallin mutants maintain their β-sheet content although it is somewhat diminished for I4F/V76D. In contrast, the near-UV CD spectrum (Figure 2B) reports significant alterations in the tertiary structure specifically in the environment of aromatic amino acids. These are more accentuated for the V76D and the double mutant I4F/V76D consistent with the expected disruptive effects of a charged residue in the protein hydrophobic core.

That these mutations destabilize γD-crystallin is evident in denaturant unfolding curves (Figure 3). At 25 °C, left shifts relative to the WT are observed in the low denaturant region leading to biphasic curves. The presence of an unfolding intermediate, hereafter referred to as I, is manifested by a plateau in the 0.5–2.5 M GdnHCl range. Mutations in γ-crystallin N-terminal domain, including V76D, have been shown to stabilize an intermediate with an unfolded N-terminal domain [37]. The midpoint of the transition from the native state, N, to I shifts to lower denaturant concentrations in the mutants relative to the WT with the largest shift observed for the double mutant. The second transition in the unfolding curves obtained at higher denaturant concentrations reflects destabilization of the C-terminal domain leading to a globally unfolded state, U. Thus, Figure 3A demonstrates that I4F and V76D destabilize the native state (N) relative to an intermediate with an unfolded N-terminus. The combination of the two mutations which are in close proximity in the three dimensional structure (Figure 1) further destabilizes N. Table 1 reports the free energy, ΔG^0, associated with each transition and the dependence of ΔG^0 on denaturant concentration, m. Because the WT unfolding curve does not have two explicit transitions, the fit errors in ΔG^0 are

considerable. In contrast, the parameters for the mutants are more narrowly defined revealing that the V76D substitution is more destabilizing than the I4F substitution.

As expected, stabilities of WT and mutants γ-crystallin are further reduced at the physiological temperature of 37 °C (Table 1). The midpoints for both transitions, from N to I and I to U, shift to lower denaturant concentrations. At this temperature, the native state of the double mutant is marginally stable. The equilibrium constant for the first transition, [I]/[N], is 0.014 suggesting that I is relatively populated even in the absence of denaturant (by comparison the fraction of U is on the order of 10^{-7}).

3.3 α-crystallins interactions with γD-crystallin mutants

Neither αA-crystallin nor αB-crystallin chaperone binds WT γD-crystallin at detectable level; even at high concentrations and molar ratios (data not shown). Furthermore, only marginal binding by αA-crystallin was detected for each of the single mutants (Figure 4A). Thus, the I4F and V76D mutations which destabilize the native state relative to the intermediate do not cross the energetic threshold for stable binding to the α-crystallin subunits.

Further destabilization of γD-crystallin native state by the combination of I4F and V76D is sufficient to promote stable binding to αA-crystallin. As previously described [28], complex formation between α-crystallin and bimane-labeled substrates changes the intensity and/or wavelength of the bimane group. Figure 4A compares the binding levels of the three mutants. Although the fluorescence of I4F and V76D changes upon addition of α-crystallin, the data is scattered and does not trace the shape of a binding isotherm indicating weak binding despite the high concentrations of γD-crystallin single mutants (50 μM compared to 25 μM for the double mutant) and large molar excess of αA-crystallin. In contrast, large and consistent changes in bimane intensity are observed for the double mutant as a function of increasing αA-crystallin molar excess. The binding isotherm can be fit assuming that α-crystallin binds only through its high affinity mode [28], i.e. with a ratio of 4 αA subunits to each γ-crystallin subunit. The complexes between α-crystallin and γD-crystallin formed within two hours of incubation at 37 °C and binding did not increase with longer incubation times (Supplementary Figure 2).

While the double mutant did not effectively bind αB-crystallin, it formed stable complexes with its phosphorylation mimic (Figure 4B). Phosphorylation of αB-crystallin at serines 15, 45 and 59 [38] enhances binding by shifting the equilibrium of Equation 2 (Scheme 1) towards an activated chaperone form [30]. Substitution of these residues by aspartates to generate αB-D3 mimics phosphorylation's effects on αB-crystallin oligomer equilibrium and chaperone activity. Binding of γD-crystallin mutants to αB-D3 produced a marginal change in intensity. Therefore, complex formation was detected through changes in bimane anisotropy. Molar excess of αB-D3 leads to a progressively larger anisotropy of bimane-labeled γD-crystallin due to the expected larger size of the complex between the two proteins. Similar to αA-crystallin, binding of the double mutant was more robust than the single mutants (data not shown) although the dissociation constant was smaller than that obtained with αA-crystallin indicating higher affinity.

3.4 Analysis of the α-crystallin/γ-crystallin complex by size exclusion chromatography

The binding trends described above were verified by size exclusion chromatography. Binding of monomeric γD-crystallin to the oligomeric α-crystallin shifts the bimane fluorescence to shorter retention times due to the larger mass of the complex [39]. For high affinity binding, the retention times are close to those of α-crystallin while for low affinity

binding, the chaperone/substrate complex runs at the void volume of a superose 6 column [16].

Figure 5A shows that incubation of αA-crystallin with WT γD-crystallin or the single mutants I4F (data not shown) and V76D does not result in detectable binding. In contrast, incubation with the double I4F/V76D leads to the concomitant reduction in the γ-crystallin peak intensity (both absorbance and fluorescence) and appearance of a fluorescence peak migrating with a retention time similar to the chaperone. This indicates the formation of a stable complex between the two proteins. At large molar excess of αA-crystallin, the binding is manifested by a distinct change in the shape of its UV absorbance peak.

Figure 5B compares the binding of γD-crystallin mutants to αB-crystallin and its phosphorylation mimic αB-D3. A 50-fold excess of αB-crystallin is required to detect fluorescence of the complex migrating at retention times similar to the αB-crystallin peak. In agreement with the conclusion of Figure 4, SEC analysis indicates that αB-D3 has the highest affinity to the γD-crystallin mutants showing detectable binding even for the two single mutants (Figure 5B). The αB-D3/γD complex is detectable by absorbance at 280 nm through a distinct peak running as a shoulder to the αB-D3 peak indicating an apparent larger size for the complex as expected (Arrows in Figures 5B and 5C).

4. Discussion

Although previous studies investigated α-crystallin suppression of γ-crystallin thermally-induced aggregation, the data presented here is the first direct quantitation of binding between the two proteins under conditions where γ-crystallin native state is more energetically favorable than its intermediate or unfolded states. We find that destabilization of γD-crystallin induces binding to α-crystallin. In addition, the stability of the α-crystallin/γ-crystallin complex evidenced by size exclusion chromatography confirms that the interaction between the two proteins is driven by α-crystallin chaperone activity. However, despite the perturbation of the native structure, binding levels for the single mutants I4F and V76D are low suggesting that destabilization by these mutations is not sufficient to trigger binding. This is unexpected considering the disruption of the tertiary structure by V76D, manifested by the near-UV CD spectrum, and the marginal stability of its native state at 37 °C (Table 1).

To frame these results into a more general context, it is instructive to compare the binding characteristics of the γD-crystallin mutants to the only other protein to which α-crystallin apparent affinity was extensively characterized, T4 Lysozyme (T4L). Similar to γD-crystallin, T4L is a highly stable protein with ΔG_{unf} of 15 kcal/mol [31]. Mutations that reduce stability were found to trigger binding to sHSP despite limited structural perturbation of the native state [31]. Apparent dissociation constants of T4L binding to α-crystallin are at least an order of magnitude smaller than those measured for the most destabilized γD-crystallin mutant investigated here, I4F/V76D [28,40]. Weak affinities to α-crystallin were also observed for βB1-crystallin mutants and attributed to the population of a dimeric intermediate with low affinity to α-crystallin [41]. Together, these results suggest that interaction between lens proteins and α-crystallin in the “chaperone mode” departs from the mechanistic principles deduced from studies of model substrates.

The γD-crystallin mutants studied here shift the unfolding equilibrium towards I. Table 1 shows that to a first approximation $\Delta G^0_{N\rightarrow I}$ decreases while $\Delta G^0_{I\rightarrow U}$ remains relatively constant. To illustrate the effects of changes in $\Delta G^0_{N\rightarrow I}$ on the fractional population of N, I and U, we carried out simulations based on a three-state equilibrium (Figure 6). Unlike a two-state folding equilibrium, the increase in the population U upon destabilization of N is

scaled by the equilibrium constant of the second transition, $K_{I\rightarrow U}$, which for γ-crystallin is much smaller than 1. Thus, the fractional population of U remains negligible (Figure 6A). Figure 6B demonstrates that significant population of U requires a reduction in the value of $\Delta G^0_{I\rightarrow U}$ which for γD-crystallin describes the unfolding of the C-terminal domain.

The coupled model of sHSP chaperone activity (Scheme 1) predicts that shift in the substrate folding equilibrium triggers binding if it increases the population of a substrate state recognized by the sHSP. Thus, the relatively large dissociation constants suggest that the γD-crystallin intermediate, I, has low affinity to α-crystallin. We conclude that similar to T4L [40], α-crystallin high affinity binding requires global unfolding of γD-crystallin.

The central finding of this paper is that a subclass of destabilizing, cataract-linked mutants of γ-crystallin can escape detection, binding and sequestration by α-crystallin. While α-crystallin binding to destabilized proteins has been extensively studied using model substrates, the results reported here suggest that conclusions based on these studies are not directly extendable to lens proteins. Each mutation or modification has to be investigated in the context of the proper unfolding equilibrium and a quantitative analysis of binding carried out. Another critical and confounding factor not addressed here is molecular crowding [42] which has been invariably neglected regardless of substrate identity or the method of its destabilization. Crowding in lens fiber cells is more peculiar involving the three molecules whose interaction is to be studied. The results presented here suggest that a detailed understanding of these molecular interactions may not be readily derived from *in vitro* studies. Thus analysis of these interactions would require adequate cellular and/or organism models that better capture the intricacies of the protein environment in lens fiber cells. Finally, our findings may have direct relevance to age-related cataract. It is possible that age-related modifications of γ-crystallins, that likewise selectively stabilize I, fail to interact with α-crystallin allowing them to nucleate aggregation.

Supplementary Material

Refer to Web version on PubMed Central for supplementary material.

Acknowledgments

The authors thank Edward Monson for technical assistance and Hanane Koteiche for critically reading the manuscript. This work was supported by Grants EY12018 and P30EY008126 from the National Institutes of Health.

Abbreviations

αB-D3	αB-crystallin S19D/S45D/S59D
GdnHCl	guanidine hydrochloride
sHSP	small heat-shock proteins
T4L	T4 lysozyme
WT	wild type

References

[1]. Bloemendal H, de Jong W, Jaenicke R, Lubsen NH, Slingsby C, Tardieu A. Ageing and vision: structure, stability and function of lens crystallins. Progress in Biophysics & Molecular Biology. 2004; 86:407–85. [PubMed: 15302206]

[2]. Wistow GJ, Piatigorsky J. Lens crystallins: the evolution and expression of proteins for a highly specialized tissue. Annual Review of Biochemistry. 1988; 57:479–504.

[3]. Benedek GB. Theory of transparency of the eyes. Appl. Opt. 1971; 10:459. [PubMed: 20094474]

[4]. Tardieu A. α-Crystallin quaternary structure and interactive properties control eye lens transparency. International Journal of Biological Macromolecules. 1998; 22:211–7. [PubMed: 9650075]

[5]. Hanson SR, Hasan A, Smith DL, Smith JB. The major in vivo modifications of the human water-insoluble lens crystallins are disulfide bonds, deamidation, methionine oxidation and backbone cleavage. Experimental Eye Research. 2000; 71:195–207. [PubMed: 10930324]

[6]. Sharma KK, Santhoshkumar P. Lens aging: effects of crystallins. Biochimica et Biophysica Acta. 2009; 1790:1095–108. [PubMed: 19463898]

[7]. David LL, Azuma M, Shearer TR. Cataract and the acceleration of calpain-induced β-crystallin insolubilization occurring during normal maturation of rat lens. Investigative Ophthalmology & Visual Science. 1994; 35:785–93. [PubMed: 8125740]

[8]. Santhoshkumar P, Raju M, Sharma KK. alphaA-crystallin peptide SDRDKFVIFLDVKHF accumulating in aging lens impairs the function of alpha-crystallin and induces lens protein aggregation. PLoS ONE [Electronic Resource]. 2011; 6:e19291.

[9]. Ortwerth BJ, James HL, Ortwerth BJ, James HL. Lens proteins block the copper-mediated formation of reactive oxygen species during glycation reactions in vitro. Biochemical & Biophysical Research Communications. 1999; 259:706–10. [PubMed: 10364483]

[10]. Nagaraj RH, Linetsky M, Stitt AW. The pathogenic role of Maillard reaction in the aging eye. Amino Acids. in press.

[11]. Truscott RJW. Age-related nuclear cataract-oxidation is the key. Experimental Eye Research. 2005; 80:709–25. [PubMed: 15862178]

[12]. Lampi KJ, Amyx KK, Ahmann P, Steel EA. Deamidation in human lens betaB2-crystallin destabilizes the dimer. Biochemistry. 2006; 45:3146–53. [PubMed: 16519509]

[13]. Asherie N, Pande J, Lomakin A, Ogun O, Hanson SR, Smith JB, Benedek GB. Oligomerization and phase separation in globular protein solutions. Biophysical Chemistry. 1998; 75:213–27. [PubMed: 9894340]

[14]. Benedek GB. Cataract as a protein condensation disease: the Proctor Lecture. Investigative Ophthalmology & Visual Science. 1997; 38:1911–21. [PubMed: 9331254]

[15]. Pande A, et al. Molecular basis of a progressive juvenile-onset hereditary cataract. Proceedings of the National Academy of Sciences of the United States of America. 2000; 97:1993–8. [PubMed: 10688888]

[16]. McHaourab HS, Godar JA, Stewart PL. Structure and mechanism of protein stability sensors: chaperone activity of small heat shock proteins. Biochemistry. 2009; 48:3828–37. [PubMed: 19323523]

[17]. Horwitz J. α-crystallin can function as a molecular chaperone. Proceedings of the National Academy of Sciences of the United States of America. 1992; 89:10449–53. [PubMed: 1438232]

[18]. Horwitz J. The function of α-crystallin in vision. Seminars in Cell and Developmental Biology. 2000; 11:53–60. [PubMed: 10736264]

[19]. Roy D, Spector A. Absence of low-molecular-weight alpha crystallin in nuclear region of old human lenses. Proceedings of the National Academy of Sciences of the United States of America. 1976; 73:3484–7. [PubMed: 1068460]

[20]. Spector A, Roy D. Disulfide-linked high molecular weight protein associated with human cataract. Proceedings of the National Academy of Sciences of the United States of America. 1978; 75:3244–8. [PubMed: 277922]

[21]. Jaenicke R, Slingsby C. Lens Crystallins and their Microbial Homologs: Structure, Stability and Function. Critical Reviews in Biochemistry and Molecular Biology. 2001; 36:435–499. [PubMed: 11724156]

[22]. Basak A, Bateman O, Slingsby C, Pande A, Asherie N, Ogun O, Benedek GB, Pande J. High-resolution X-ray crystal structures of human gammaD crystallin (1.25 A) and the R58H mutant (1.15 A) associated with aculeiform cataract. Journal of Molecular Biology. 2003; 328:1137–47. [PubMed: 12729747]

[23]. Slingsby C, Clout NJ. Structure of the crystallins. Eye. 1999; 13:395–402. [PubMed: 10627816]

[24]. Banerjee PR, Pande A, Patrosz J, Thurston GM, Pande J. Cataract-associated mutant E107A of human gammaD-crystallin shows increased attraction to alpha-crystallin and enhanced light scattering. Proceedings of the National Academy of Sciences of the United States of America. 2011; 108:574–9. [PubMed: 21173272]

[25]. Pande A, Ghosh KS, Banerjee PR, Pande J. Increase in surface hydrophobicity of the cataract-associated P23T mutant of human gammaD-crystallin is responsible for its dramatically lower, retrograde solubility. Biochemistry. 2010; 49:6122–9. [PubMed: 20553008]

[26]. Liu H, et al. Crystallin {gamma}B-I4F mutant protein binds to {alpha}-crystallin and affects lens transparency. Journal of Biological Chemistry. 2005; 280:25071–8. [PubMed: 15878859]

[27]. Wang K, et al. GammaD-crystallin associated protein aggregation and lens fiber cell denucleation. Investigative Ophthalmology & Visual Science. 2007; 48:3719–28. [PubMed: 17652744]

[28]. Sathish HA, Stein RA, Yang G, Mchaourab HS. Mechanism of chaperone function in small heat-shock proteins. Fluorescence studies of the conformations of T4 lysozyme bound to alphaB-crystallin. J. Biol. Chem. 2003; 278:44214–44221. [PubMed: 12928430]

[29]. Jung J, Byeon IJ, Wang Y, King J, Gronenborn AM. The structure of the cataract-causing P23T mutant of human gammaD-crystallin exhibits distinctive local conformational and dynamic changes. Biochemistry. 2009; 48:2597–609. [PubMed: 19216553]

[30]. Koteiche HA, McHaourab HS. Mechanism of chaperone function in small heat-shock proteins. Phosphorylation-induced activation of two-mode binding in alphaB-crystallin. Journal of Biological Chemistry. 2003; 278:10361–7. [PubMed: 12529319]

[31]. Mchaourab HS, Dodson EK, Koteiche HA. Mechanism of Chaperone Function in Small Heat-Shock Proteins.Two-Mode Binding of the Excited States of T4 Lysozyme Mutants by aA-Crystallin. Journal of Biological Chemistry. 2002; 277:40557–40566. [PubMed: 12189146]

[32]. Berengian AR, Bova MP, Mchaourab HS. Structure and function of the conserved domain in αA-crystallin. Site-directed spin labeling identifies a β-strand located near a subunit interface. Biochemistry. 1997; 36:9951–7. [PubMed: 9296605]

[33]. Horwitz J, Huang QL, Ding L, Bova MP. Lens α-crystallin: chaperone-like properties. Methods in Enzymology. 1998; 290:365–83. [PubMed: 9534176]

[34]. Eftink MR. The use of fluorescence methods to monitor unfolding transitions in proteins. Biochemistry-Russia. 1998; 63:276–84.

[35]. Shashidharamurthy R, Koteiche HA, Dong J, McHaourab HS. Mechanism of chaperone function in small heat shock proteins: dissociation of the HSP27 oligomer is required for recognition and binding of destabilized T4 lysozyme. Journal of Biological Chemistry. 2005; 280:5281–9. [PubMed: 15542604]

[36]. Koteiche HA, McHaourab HS. Mechanism of a Hereditary Cataract Phenotype: Mutations in αA-crystallin activate substrate binding. Journal of Biological Chemistry. 2006; 281:14273–9. [PubMed: 16531622]

[37]. Moreau KL, King J. Hydrophobic core mutations associated with cataract development in mice destabilize human gammaD-crystallin. Journal of Biological Chemistry. 2009; 284:33285–95. [PubMed: 19758984]

[38]. Ito H, Kamei K, Iwamoto I, Inaguma Y, Nohara D, Kato K. Phosphorylation-induced change of the oligomerization state of αB-crystallin. Journal of Biological Chemistry. 2001; 276:5346–52. [PubMed: 11096101]

[39]. Sathish HA, Koteiche HA, McHaourab HS. Binding of destabilized betaB2-crystallin mutants to alpha-crystallin: the role of a folding intermediate. Journal of Biological Chemistry. 2004; 279:16425–32. [PubMed: 14761939]

[40]. Claxton DP, Zou P, McHaourab HS. Structure and orientation of T4 lysozyme bound to the small heat shock protein alpha-crystallin. Journal of Molecular Biology. 2008; 375:1026–39. [PubMed: 18062989]

[41]. Mchaourab HS, Kumar MS, Koteiche HA. Specificity of alphaA-crystallin binding to destabilized mutants of betaB1-crystallin. FEBS Letters. 2007; 581:1939–43. [PubMed: 17449033]

[42]. Minton AP. The influence of macromolecular crowding and macromolecular confinement on biochemical reactions in physiological media. Journal of Biological Chemistry. 2001; 276:10577–80. [PubMed: 11279227]

- How can destabilizing mutations of lens γ-crystallin cause cataract?
- We characterize the unfolding equilibrium of two cataract-causing mutations and investigate their interactions with α-crystallins
- Cataract-causing mutations stabilize an unfolding intermediate of γD-crystallin
- Cataract-causing mutants of γD-crystallin are not efficiently bound by lens α-crystallin
- Destabilized variants of γD-crystallin, due to mutations or age-related modifications, can nucleate aggregation leading to lens opacity and cataract

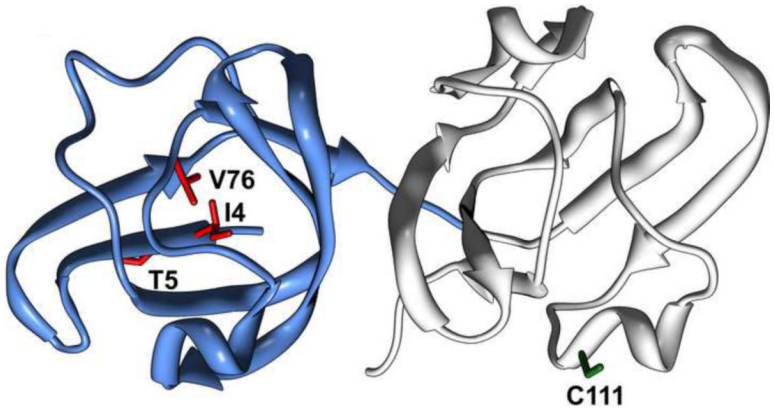

Figure 1.
Ribbon representation of γD-crystallin structure (pdbID 1HK0). The N-terminal domain is colored in blue; sites of cataract-causing mutations are highlighted in red and cysteine 111 in green.

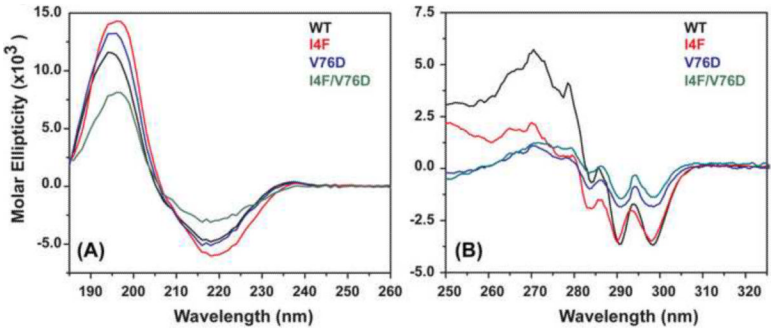

Figure 2.

Room temperature CD analysis of γD-crystallin mutants. (A) Far-UV spectra showing a pronounced minimum at 218 nm. (B) Near-UV spectra reporting changes in the tertiary fold as a consequence of the mutations.

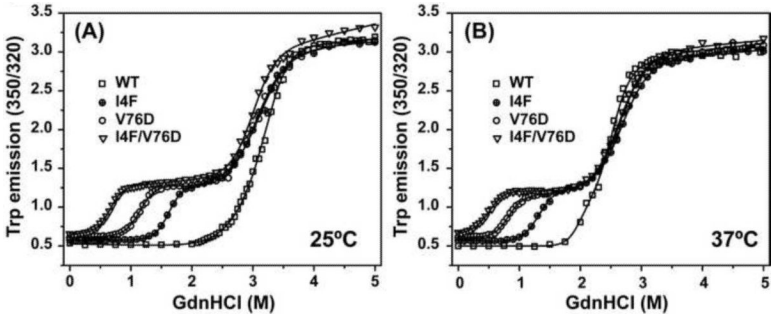

Figure 3.

Denaturant unfolding curves of γD-crystallin mutants at (A) 25 °C and (B) 37 °C. The substitutions lead to the appearance of two explicit transitions compared with the WT monophasic curve. The first transition corresponds to the population of an intermediate with an unfolded N-terminal domain. The second transition corresponds to unfolding of the C-terminal domain. The solid lines represent non-linear least-squares fit yielding the parameters reported in Table 1.

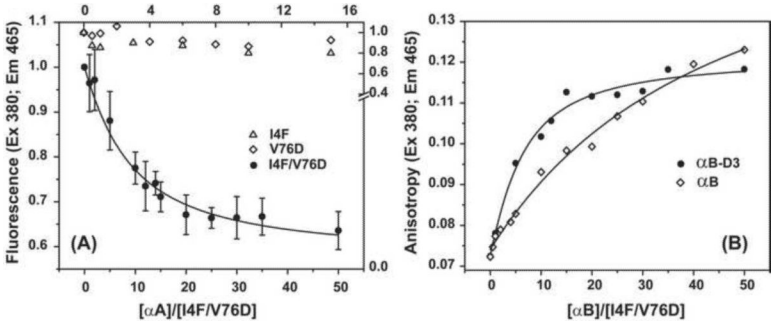

Figure 4.

Binding isotherms of γD-crystallin mutant to (A) αA-crystallin and (B) αB-crystallin and its phosphorylation mimic αB-D3. The concentration of the single mutants was 50 μM while the double mutant was 25 μM. Samples were incubated at 37 °C for two hours at the appropriate ratio as described in the methods section. The solid lines for the double mutant I4F/V76D in (A) and (B) are non-linear least-squares fit assuming high affinity binding where 4 α-crystallin subunits bind one γ-crystallin. The dissociation constants are 43±7 and 27±6 μM for αA-crystallin and αB-D3, respectively. For αB-crystallin, the dissociation constant was larger than 300 μM.

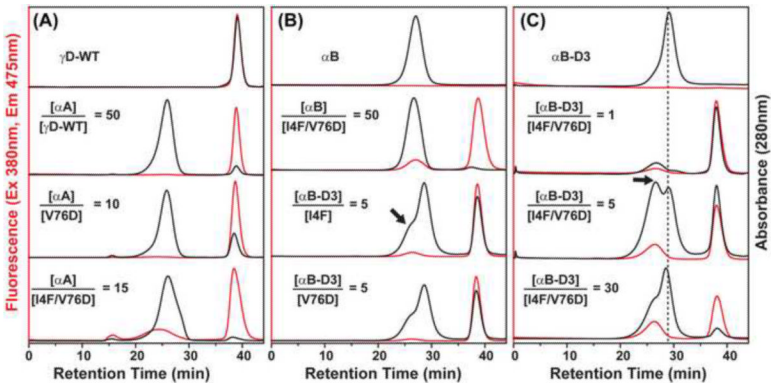

Figure 5.

Analysis of γD-crystallin mutant binding to α-crystallin by size exclusion chromatography (SEC) detected by in-line absorbance at 280 nm and fluorescence at 475 nm. (A) Samples of αA-crystallin and γD-crystallin were incubated at the indicated molar ratios and injected on a Superose 6 column. The binding of γD-crystallin I4F/V76D is manifested by a fluorescence peak with retention time similar to that of αA-crystallin. (B) Comparative SEC analysis of binding to αB-crystallin and αB-D3. A 50-fold molar excess of the former is required for detectable binding of the double mutant while αB-D3 binds the single mutants. The y axes were scaled to show details of the complex peak. (C) The complex between αB-D3 and γD-crystallin is detected as a distinct peak, indicated by the arrow, migrating at a larger mass than αB-D3 alone.

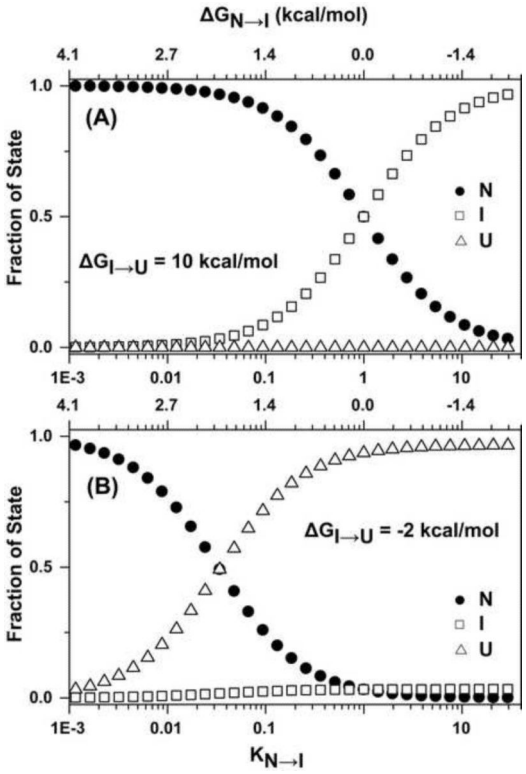

Figure 6.

Fraction of N, I and U as a function of changes in $\Delta G^0_{N\rightarrow I}$ for (A) $\Delta G^0_{I\rightarrow U}$ = 10 kcal/mol and (B) $\Delta G^0_{I\rightarrow U}$= −2 kcal/mol. For (B) shifts in the $\Delta G^0_{N\rightarrow I}$ lead to a large increase in the fraction of U. These simulations apply to three-state unfolding equilibria.

$$N \rightleftharpoons I \rightleftharpoons U \quad [1]$$

$$sHSP \rightleftharpoons (sHSP)_a \quad [2]$$

$$(sHSP)_a + I/U \rightleftharpoons C_{I/U} \quad [3]$$

scheme 1.

Table 1

Equilibrium unfolding/refolding parameters for γD-crystallin wild-type and mutants at pH 7.2

γD-crystallin	Temperature	N ⇌ I			I ⇌ U		
		$\Delta G^0_{N\rightarrow I}$	m	$C_{½}$	$\Delta G^0_{I\rightarrow U}$	m	$C_{½}$
	°C	kcal/mol	kcal/mol/M	M	kcal/mol	kcal/mol/M	M
WT	25	6.23 ± 17.9	2.08 ± 3.90	2.74	10.4 ± 24.1	3.12 ± 6.77	3.24
	37	10.7 ± 18.7	5.46 ± 9.46	2.03	10.3 ± 3.88	4.08 ± 1.60	2.51
I4F	25	8.50 ± 2.18	5.26 ± 1.39	1.58	7.67 ± 1.30	2.48 ± 0.40	3.00
	37	5.99 ± 0.78	4.52 ± 0.62	1.35	7.56 ± 0.62	2.83 ± 0.23	2.65
V76D	25	5.48 ± 0.66	4.71 ± 0.58	1.18	7.85 ± 0.77	2.59 ± 0.25	2.96
	37	4.36 ± 0.92	5.38 ± 1.08	0.79	8.14 ± 0.84	3.07 ± 0.31	2.55
I4F/V76D	25	3.96 ± 0.62	5.99 ± 0.83	0.62	9.68 ± 1.04	3.24 ± 0.35	2.79
	37	2.67 ± 0.54	5.07 ± 0.74	0.50	7.37 ± 0.36	2.81 ± 0.13	2.59

ΔG^0, m, and $C_{½}$ are the free energy, the denaturant dependence of ΔG^0, and the concentration of urea at the transition midpoint, respectively, for the two transitions of γD-crystallin unfolding. ΔG^0, m are reported with the associated fit error.